

# Constraining Dislocation Movement in Molecular Dynamics: Application to Crack-dislocation Interactions.

D. Tanguy<sup>1</sup>

*CNRS, UMR 5146, Ecole des Mines de Saint-Etienne, centre SMS,  
158 cours Fauriel, F-42023 Saint-Etienne, France.*

## Abstract:

Modeling semi-brittle fracture is a multiscale task. A first approach could be made in two dimensions by coupling discrete dislocation dynamics (DD) and molecular dynamics (MD). The problem is that dislocations are not static in MD whereas, in DD, equilibrium elastic solutions and superposition are usually used. We have recently proposed new equations of motion for MD which give full control on dislocation mobility. An order parameter is used to measure the local shear and use it as a holonomic constraint, in the same spirit as the constraints used in the dynamics of molecules with rigid bonds. In this paper, we show two applications: constraining dislocation emission from a crack tip (intrinsic ductility) and the calculation of crack tip shielding from a pinned dislocation. We show that DD and MD are in excellent agreement, which opens the possibility of studying complex dislocation – crack tip arrangements, multiscale.

## 1. Introduction

Crack propagation does not occur in ductile crystals (austenitic stainless steels, aluminum and nickel based alloys) under tensile load. They fail, after a large, irreversible, deformation by coalescence of voids and intense, localized, plastic shear. On the contrary, when degradation from the environment occurs (irradiation, H embrittlement, liquid metal embrittlement), a crack might nucleate at the surface and propagate through the crystal, either because of embrittlement by adsorption at the tip or by solute segregation at defects ahead of the tip, like interfaces. Another important class of solids is those which exhibit a brittle to ductile transition (BDT), like body centered cubic crystals (ferritic steels,  $\beta$  titanium) or silicon. In this case, the response of the material to an external load is largely dominated either by dislocation mobility or multiplication. At low temperature, thermal activation is not efficient enough to enable dislocation movement and the system relaxes its elastic energy by propagating a crack. At high temperature, dislocations are emitted and arrange in such a way as to release the elastic energy. The transition between these two behaviors is usually not sharp [1], at a definite temperature ( $T_c$ ), when the system contains enough built in dislocations that can act as sources. It means that within a temperature window around  $T_c$ , these materials could also develop brittle cracks in a noticeably ductile matrix. Therefore, both problems (environment degradation and BDT) rely on the

---

<sup>1</sup> E-mail: [tanguy@emse.fr](mailto:tanguy@emse.fr)

same basic situation: a loaded crack tip in interaction with a collection of dislocations.

Our approach of the simulation of this situation is somewhat "radical" in the sense that we believe that crack-dislocation interactions should be modeled at a mesoscale, using elasticity theory (and, if possible, discrete dislocations), whereas crack tip phenomena should be treated at the atomic scale by MD. It means that dislocation nucleation during crack propagation should be forbidden in MD simulations (blunting can be taken into account), except when dealing the specific problem of emission from the tip. This because MD box are not large enough and the time scales are too short to handle the formation of a dislocation microstructure. To achieve this decoupling, we derive equations of motion which incorporate a constraint in order to control dislocation activity (nucleation and mobility) in MD simulations. These are used only to measure some quantities characteristic of the fracture process at the tip that can be transferred to higher scales, as shown below.

The connection between atomistics and the mesoscale (from the nm to 10 $\mu$ m, in 2D) relies on the powerful results of the continuum theory of cracks. Linear elasticity and complex analysis provide analytical solutions for the stress fields valid in all space, in the presence of dislocations [2] (in 2D). The first major result is the universal shape of the asymptotic fields close to the tip:

$$\sigma_{zz} = \frac{k}{\sqrt{2\pi r}} f(\theta) \quad (1)$$

where the dependence on the remote load, boundary shapes, crack length are all included in the single scalar  $k$  called the stress intensity factor. For example, for a flaw of length  $2a$ , in an infinite medium, loaded by a stress  $\sigma$ :  $k = \sigma\sqrt{\pi a}$ .

When dislocations are present,  $k$  depends on the configuration i.e. on the set of dislocation positions, but Eq.1 is still valid. In this case,  $k$  is referred to as the "local  $k$ " and the applied load as  $K_{\text{applied}}$  [2].  $K_{\text{applied}}$  is the stress intensity factor that the crack would undergo from the remote load if there were no dislocations. The crack is said to "shielded" if  $k < K_{\text{applied}}$ . The second important result is the connection with the elastic energy release rate  $G$  (the variation of the stored elastic energy with the crack length):  $G = k^2/E'$ , where  $E'$  is an elastic constant.

For a perfect brittle crack propagation, where the shape of the crack remains self-similar, the Griffith energy balance provides a fracture criterion:  $2\gamma_s = G = k_{IG}^2/E'$ ,

where  $2\gamma_s$  is the excess energy of the newly created surfaces. In the same spirit, we perform intensive quenched molecular dynamics simulations at increasing levels of load, measure  $k$  and detect the critical  $k$  values for the elementary processes at the tip:  $k_{Ic}$  for cleavage,  $k_{Ie}$  for dislocation emission,  $k_{Iv}$  for nucleation of vacancies... If the "local  $k$ " concept holds, these values could be incorporated in mesoscale simulations.

In this paper, we recall the derivation of the equations for constrained molecular dynamics (CMD) and apply them: first in a system containing a crack alone, getting access to numerical values for  $k_{Ic}$ ,  $k_{Ie}$  and  $k_{Iv}$ ; second, in the case where a

single dislocation interacts with a crack. The constrains are applied at increasing distances from the crack tip where the dislocation is pinned. The stress calculation at the atomic scale shows how much shielding is provided by the dislocation as a function of its distance to the tip, which, compared to the elastic solution, provides a test of the local k concept. Finally, we briefly expose the principle of a discrete dislocation dynamics (DDD) simulation, just to give a first example of how the critical k can be used at the mesoscale. All the details concerning the different methods can be found in references [3-5]. Here, the emphasis is on making the link between them.

## 2. Constrained molecular dynamics

In order to control the dislocation activity, the local shear (the non elastic perturbation of the environment left along the glide plane by the displacement of the defect) has to be measured by an order parameter. We use a centrosymetry parameter  $CS_i$ , inspired by [6]:

$$CS_i = \left( \sum_j \vec{q}_j - \vec{q}_i + \vec{q}_{j+6} - \vec{q}_i \right) \cdot \vec{b} \quad (2)$$

where  $i$  is the label of the particle where the local shear is evaluated and  $j$  is the label of its first neighbors, in the undeformed structure. The vectors  $\vec{q}$  are the positions of the particles. The labels  $j$  and  $j+6$  refer to a pair of opposite first neighbors in the undeformed structure of a centrosymmetric crystal, like fcc. Finally, the vectorial sum over all the pairs is projected on the glide direction  $\vec{b}$ .  $\vec{b}$  is known a priori, from crystallography (for example, the 12 Shockley partial orientations in fcc). This order parameter is very close to zero when the structure is only elastically deformed and takes a large value, close to  $mb^2$  when a dislocation of Burgers vector  $b$  has sheared its local environment.  $m$  is the number of first neighbour pairs which are sheared by the dislocation. For example,  $m=3$  for a glide along a  $\{111\}$  plane in fcc.

Then, the constraint is:

$$CS_i < CS \quad (3)$$

where  $CS$  is a constant threshold, higher than the variations of  $CS_i$  due to the elastic deformations alone. If  $n$  particles are constrained, Eq.3 form a set of coupled equations which depend only on positions: holonomic constraints. Following [7, 8], equations of motions are derived [3] which incorporate these constraints by means of Lagrange multipliers. The additional term they contain is a configurational force aligned along the glide direction specified by  $\vec{b}$  in Eq.2. We recall that holonomic constraints don't produce any work. This property is

interesting, as shown in the next paragraph, when the method is used to constrain crack tips in order to study purely brittle crack propagation.

A first application is the quantification of the intrinsic ductility versus brittleness of a material. Consider a crack (Fig.1), in an fcc single crystal, lying along a  $\{111\}$  plane, with a crack front lying along  $\langle 110 \rangle$ , loaded in traction (mode I). In this orientation, most fcc crystals are intrinsically ductile (except pathological cases like Iridium) which means that a dislocation is spontaneously emitted from the crack tip at a critical load. It is not possible to explore the brittle configurations in that case, which are clearly not physical, but nevertheless interesting if one wants to know how much the cohesion should be decreased (by impurity segregation for example) in order to get a transition from intrinsic ductility to brittleness [9]. By constraining the particles in the vicinity of the crack tip (light gray particles on Fig.1b), such brittle configurations can be explored. In the calculations of Fig.1, the traction is applied by a rigid displacement at the border of the box. This is not an efficient way to characterize the load at the crack tip. As explained in the introduction, it is more convenient to use the stress intensity factor. Following [10], we measure  $k$  at the tip by fitting the virial stress profile on the Inglis solution. With the interatomic potential given in [11], we observe dislocation emission at  $k_{Ie} \approx 0.64k_{IG}$ , brittle crack propagation at  $k_{Ic} \approx k_{IG}$  and also an original mechanism, where vacancies form just ahead of the crack tip, at  $k_{Iv} \approx k_{IG}$ . This last result is obtained on a blunted crack tip constrained one plane further away than the crack presented on Fig.1.

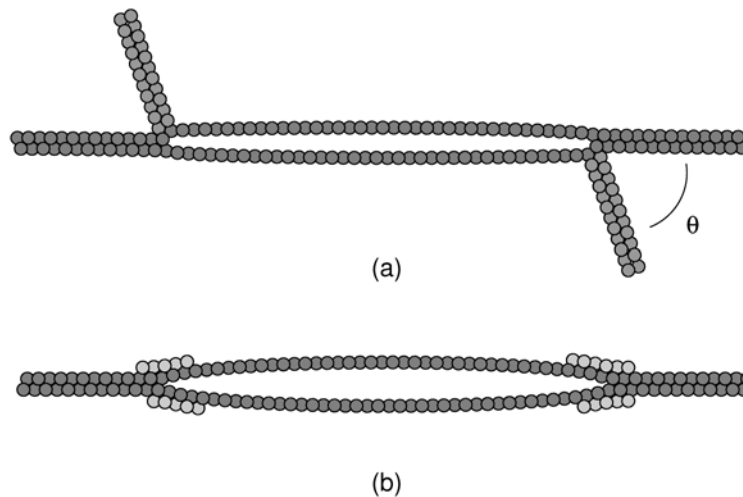


Figure 1 : (a) An intrinsically ductile crack, loaded just above  $k_{Ie}$ , emits a Shockley partial dislocation. The crack lies along a  $\{111\}$  plane in fcc with a crack front along  $\langle 110 \rangle$ . The interatomic potential is the phenomenological Al from [11]. (b) A brittle crack, loaded just above  $k_{IG}$ , propagates. The light gray particles are constrained. The potential is the same as in (a).

### 3. Crack tip shielding

We now turn to the basic concept underlying the multiscale simulation of semi-brittle cracking: the local  $k$  felt by the crack tip in the presence of a dislocation. Two twin problems are treated in parallel. The first calculation, done by CMD, concerns a nanometer scale flaw, of length  $2a=16a_0$ . The second is a semi-infinite crack in an infinite isotropic medium treated by the elastic theory [2]. To introduce a dislocation in the atomistic box, the load is increased slightly above  $k_{Ic}$  and a small mode III is added to force the emission of the second partial, whose Burgers vector is not in the plane of the figure because of the crystallographic orientation. The crucial point is to obtain static stress fields which are the one that can be compared to elasticity. As the dislocation is perfect, it is not tied to the crack tip by the stacking fault ribbon. Therefore, it should cross the box and get stuck at the border. CMD can efficiently pin the dislocation: instead of constraining particles at the immediate vicinity of the crack tip, they can be constrained at some chosen positions, further away, along the glide plane [4]. A set of positions is shown in table 1. The stress profiles computed by both methods, for these configurations, are presented in Fig.2.

Table 1 : Distances where the dislocations are pinned, along the slip plane inclined at  $\theta=70^\circ$  (zero is the tip). See figure1 for the orientation of the slip plane. The numbers given to the frames are consistent through all the figures and text.

Frame number	0	1	2	3	4	6	10
Distance ( $a_0$ )	0	3.7	7.4	11	14.7	22.1	36.8

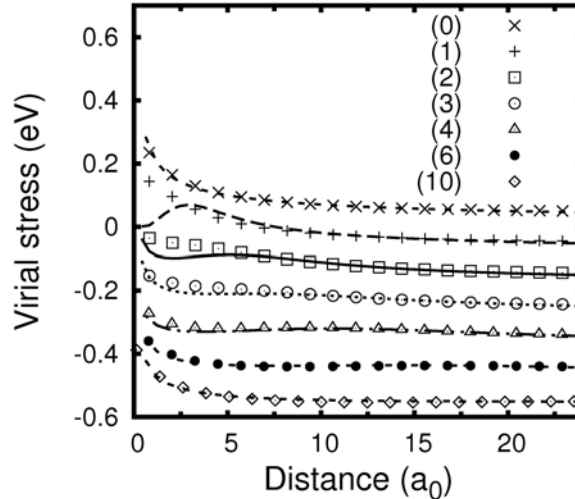


Figure 2 : Comparison of the stress profiles (multiplied by the atomic volume) (traction) obtained by CMD (symbols) and elastic calculations (lines). The positions of the dislocation are given in table 1. The frames are shifted downward by steps of 0.1eV for clarity. Multiply the stress values by 9.8 to have GPa ( $[\sigma]=1 \text{ eV}/((4.04 \text{ \AA})^3/4)=9.8\text{GPa}$ ).

On the curves (1) to (3), the agreement is bad between CMD and elasticity. The configurations correspond to the emission of the first Shockley partial with a stacking fault ribbon joining the tip. Curves (4) to (10), where the agreement is remarkable, correspond to a fully formed, perfect, dislocation. Curve (0), in Fig. 2, represents the load in the absence of dislocation and the stress singularity is characterized by  $K_{\text{applied}}$ . As the dislocation is emitted, the stress singularity is indeed decreased and the good agreement with elasticity allows the use of the analytical formulas for the computation of  $k$ . The concept of local  $k$  is therefore valid, provided the dislocation is perfect. Note that elasticity breaks down, not because of nonlinearity (the stress levels are still in the range where the potential is reasonably linear), but because of the presence of the stacking fault. The surprise is the quite large distance that must separate the crack from the dislocation in order for the analytical formulas to be valid: of the order of  $10a_0$  (Table 1), 4nm, with respect to the Burgers vector dimension.

#### 4. Discrete dislocation dynamics

The basic ingredients of the simulation are recalled. A trace of the crystalline structure is included in this continuum elasticity based simulation by fixing the orientation of the glide planes. The entire space is covered by parallel slip planes, with a spacing of the order of  $80b$ , where  $b$  is the Burgers vector of the dislocations considered. Dislocation sources are randomly distributed on these slip planes. Time  $t$  is discretized. From the value of  $K_{\text{applied}}$  at time  $t$ , the stress field can be computed at any point in space using analytical stress formulas. When the stress on a source is higher than a critical value for nucleation  $\tau_{\text{nuc}}$ , the source is activated and a dislocation dipole is emitted which, in this simple 2D model, represents the trace of a dislocation loop. Once a dislocation is emitted, it is displaced according to a velocity law:

$$\vec{v} = B\vec{f}$$

where  $\vec{f}$  is the Peach and Koelher force obtained from  $\vec{f} = \overline{\sigma} \wedge \vec{\xi}$  where  $\vec{\xi}$  is the line vector.  $B$  is a constant (viscous drag).  $\overline{\sigma}$  is the stress tensor computed from the complex potentials in [2] which included the contribution of the crack and all the dislocations. It was used previously by Chateau [12] for treating the problem of H segregation at a pile up ahead of a crack. Phenomenological rules are also applied to describe the pinning at obstacles, the line tension effect, annihilation and junction formation [13]. A dislocation structure develops in front of the crack tip, with formation of intense slip bands due to crack tip emission and activation of sources in region of high resolved shear (primary and secondary slip) [5]. Figure 3 shows the time evolution of the local  $k$  which includes the contribution of the whole dislocation structure. At early times, the local  $k$  and the applied  $K$  are the same, until emission is activated (first from the tip and then from many other sources). Emission "from the tip" occurs at  $k_{\text{le}} \approx 0.25 \text{MPa m}^{1/2}$ . The criterion

is such that a new dislocation can not be emitted until the preceding has moved away, the speed of which depends on the density of obstacles and the dislocation configuration, in particular the formation of junctions. Therefore, in between two dislocation emissions,  $K$  and  $k$  increase and  $k$  becomes higher than  $k_{Ic}$ . The critical load for brittle propagation is  $k_{Ic} \approx 0.9 \text{MPa m}^{1/2}$ , which should be reached, by extrapolation, for  $K \approx 3 \text{MPa m}^{1/2}$ . Then, in principle, the crack should be advanced by an infinitesimal amount and the local  $k$  recomputed.

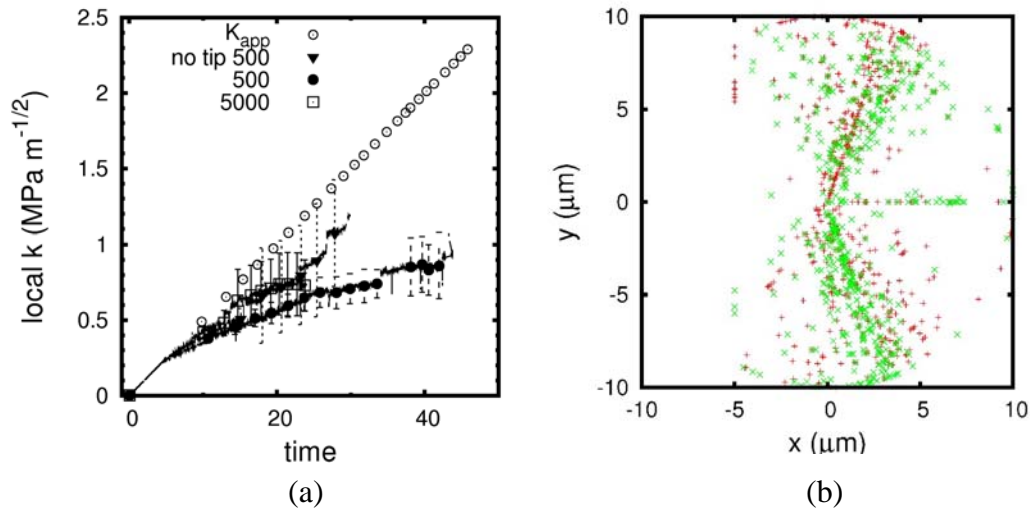


Figure 3 : (a) Time variation of  $k$  and  $K_{\text{applied}}$  obtained by discrete dislocation dynamics ; (b) a typical dislocation configuration where the crack is horizontal, coming from the left and the tip is in  $(0,0)$ . Each point represents a dislocation.

The validity of this fracture criterion, when the dislocation free zone is very small, is not clear and needs to be tested, in particular when the crack approaches a dislocation stored on the interface. Another limitation which should be lifted with more MD simulations is the crack velocity, in presence of dislocations close to the tip.

#### Acknowledgments:

This work is supported by the French Agence Nationale de la Recherche under project H-inter (number ANR-06-BLAN60231).

#### References:

- [1] S. G. Roberts, in *Multiscale Phenomena in Plasticity*, edited by J. Lépinoux, D. Mazière, V. Pontikis and G. Saada (Kluwer Academic Press, Netherlands, 2000), p. 349.
- [2] I. H. Lin and R. Thomson, *Acta Metal.* 34, 187 (1986)
- [3] D. Tanguy, *Phys. Rev. B* 76, 144115 (2007)
- [4] D. Tanguy, M. Razafindrazaka and D. Delafosse, *Acta Mater.* 56, 2441 (2008)

- [5] D. Tanguy, D. Delafosse and M. Razafindrazaka, *Acta Mater*, submitted.
- [6] C. L. Kelchner, S. J. Plimpton and J. C. Hamilton, *Phys. Rev. B* 58, 11085 (1998)
- [7] J. P. Ryckaert, G. Ciccotti and H. J. C. Berendsen, *J. Comp. Phys.* 23, 327 (1977)
- [8] H. Goldstein, *Classical Mechanics*, 2<sup>nd</sup> edition (Addison-Wesley, Reading, Mass. 1980)
- [9] J. R. Rice and R. Thomson, *Philos. Mag.* 29, 73 (1974)
- [10] A. Mattoni, L. Colombo and F. Cleri, *Phys. Rev B* 70, 094108 (2004)
- [11] A. Aslanides and V. Pontikis, *Phil. Mag. Lett.* 78, 377 (1998)
- [12] J. P. Chateau, D. Delafosse, and T. Magnin, *Acta Mater.* 50, 1523 (2002)
- [13] M. Razafindrazaka, D. Tanguy and D. Delafosse, *Mat. Sci. Eng.*, submitted.